Homozygous mutation in *SAMHD1* gene causes cerebral vasculopathy and early onset stroke

Baozhong Xin[a], Stephen Jones[b], Erik G. Puffenberger[c,d], Claas Hinze[e], Alicia Bright[a], Haiyan Tan[f], Aimin Zhou[f], Guiyun Wu[b], Jilda Vargus-Adams[e], Dimitris Agamanolis[g], and Heng Wang[a,h,i,1]

[a]DDC Clinic for Special Needs Children, Middlefield, OH 44062; [b]Department of Radiology, Cleveland Clinic, Cleveland, OH 44195; [c]The Clinic for Special Children, Strasburg, PA 17579; [d]Department of Biology, Franklin and Marshall College, Lancaster, PA 17603; [e]Department of Pediatrics, Cincinnati Children's Hospital Medical Center, Cincinnati, OH 45229; [f]Department of Chemistry, Cleveland State University, Cleveland, OH 44115; [g]Department of Pathology, Akron Children's Hospital, OH 44308; [h]Department of Pediatrics, Rainbow Babies and Children's Hospital, Cleveland, OH 44106; and [i]Department of Molecular Cardiology, Cleveland Clinic, Cleveland, OH 44195

Edited by C. Thomas Caskey, University of Texas-Houston Health Science Center, Houston, TX, and approved February 3, 2011 (received for review September 23, 2010)

We describe an autosomal recessive condition characterized with cerebral vasculopathy and early onset of stroke in 14 individuals in Old Order Amish. The phenotype of the condition was highly heterogeneous, ranging from severe developmental disability to normal schooling. Cerebral vasculopathy was a major hallmark of the condition with a common theme of multifocal stenoses and aneurysms in large arteries, accompanied by chronic ischemic changes, moyamoya morphology, and evidence of prior acute infarction and hemorrhage. Early signs of the disease included mild intrauterine growth restriction, infantile hypotonia, and irritability, followed by failure to thrive and short stature. Acrocyanosis, Raynaud's phenomenon, chilblain lesions, low-pitch hoarse voice, glaucoma, migraine headache, and arthritis were frequently observed. The early onset or recurrence of strokes secondary to cerebral vasculopathy seems to always be associated with poor outcomes. The elevated erythrocyte sedimentation rate (ESR), IgG, neopterin, and TNF-α found in these patients suggested an immune disorder. Through genomewide homozygosity mapping, we localized the disease gene to chromosome (Chr) 20q11.22-q12. Candidate gene sequencing identified a homozygous mutation, c.1411–2A > G, in the *SAMHD1* gene, being associated with this condition. The mutation appeared at the splice-acceptor site of intron 12, resulted in the skipping of exon 13, and gave rise to an aberrant protein with in-frame deletion of 31 amino acids. Immunoblotting analysis showed lack of mutant SAMHD1 protein expression in affected cell lines. The function of SAMHD1 remains unclear, but the inflammatory vasculopathies of the brain found in the patients with *SAMHD1* mutation indicate its important roles in immunoregulation and cerebral vascular hemeostasis.

genotyping | SNP arrays | autozygosity

Cerebrovascular diseases and stroke are a leading cause of death and disability in developed countries. Although they are less common in children, pediatric cerebrovascular disorders are important causes of morbidity and mortality and are increasing in prevalence (1, 2). Because of the frequent need for life-long medical services and social supports in the survivors, the implications for healthcare and social resource utilization in pediatric patients are often greater; thus, the identification of young populations at risk, early diagnosis, and appropriate management of the diseases become more important.

Increasing evidence suggests that there is a significant genetic predisposition to stroke, with more convincing findings through several single gene disorders in young patients (3). To identify these single genes and study the pathogenesis of cerebrovascular disorders caused by the alteration of these genes will not only help the disease diagnosis and treatment in the affected patients, but also potentially provide valuable information in understanding the pathophysiology of cerebrovascular diseases in general. Here we describe a cohort of patients with cerebral vasculopathy and early onset of stroke in an extended Old Order Amish pedigree. Through a genomewide homozygosity mapping study and mutational analysis, we identified a genetic variation in the *SAMHD1* gene associated with this autosomal recessive condition.

Results

Clinical Phenotype. Fourteen individuals (10 males and four females), ranging from newborn to 25 y in age, were identified with this condition. The phenotype was not observed in the parents or 21 unaffected siblings. Three full-term stillbirths, without knowledge of phenotype, were reported from two mothers. All patients demonstrated Old Order Amish ancestry, and genealogical analyses revealed multiple lines of common descent between all parents of affected children although they resided in three different states (Fig. 1).

All affected children were full term, born after an uneventful pregnancy and delivery. Routine hematologic and metabolic screenings were all within normal ranges at birth. Standard karyotype analysis was performed on at least two patients and reported as normal. Although there were no significant dysmorphic features noted at birth, the affected newborns tended to be relatively smaller for their gestational age with 13 out of 14 weighing less than the 15th percentile. Their average birth weight (2,670 ± 193 g), length (48.2 ± 1.5 cm), and occipitofrontal circumference (OFC) (32.9 ± 1.8 cm) were all in the low end of the normal range (Table S1). Thin and transparent underdeveloped skin, similar to what we might see in preterm infants, was noted in at least 7 of these newborns. Thirteen infants were thereafter included for further clinical phenotype description, whereas 1 newborn identified through DNA mutation analysis right before the end of this study was excluded because his phenotype might not be fully expressed.

The overall clinical phenotype of this condition was very heterogeneous with a wide range of clinical manifestations and considerably diverse clinical presentations, including cerebral palsy, stroke, developmental delay, failure to thrive, chilblains, and arthritis (Tables 1 and 2). More than half of the affected children were hypotonic and severely irritable during their infancy (Table 1). Failure to thrive, short stature, joint stiffness or arthritis, high-arched palate, and low-pitch hoarse voice were also observed in the majority of the affected individuals. The children tended to have poor tolerance to extreme environments, both cold and hot. Acrocyanosis was often found on their hands, feet, and face, worsening during cold weather (Raynaud's phenomenon), and eight children had a history of chilblain lesions in acral locations during winter. Migraine headache, seizure, hy-

Author contributions: B.X. and H.W. designed research; B.X., E.G.P., C.H., A.B., H.T., A.Z., J.V.-A., and H.W. performed research; B.X., S.J., E.G.P., C.H., A.B., G.W., J.V.-A., D.A., and H.W. analyzed data; and B.X. and H.W. wrote the paper.

The authors declare no conflict of interest.

This article is a PNAS Direct Submission.

[1]To whom correspondence should be addressed. E-mail: wang@ddcclinic.org.

This article contains supporting information online at www.pnas.org/lookup/suppl/doi:10.1073/pnas.1014265108/-/DCSupplemental.

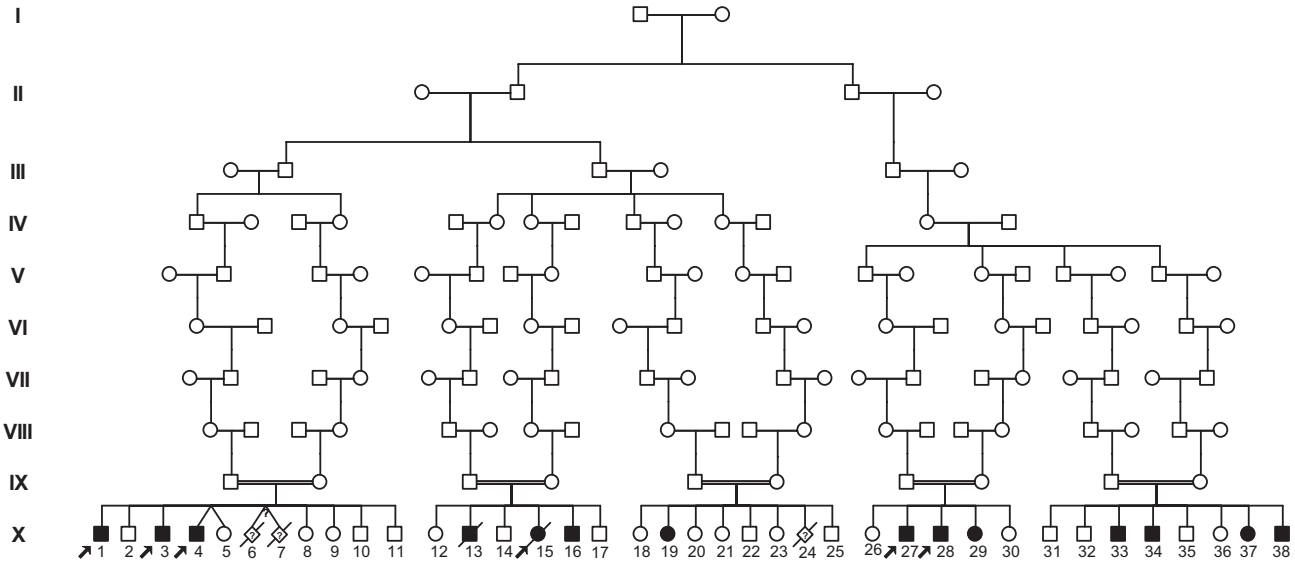

Fig. 1. Partial pedigree of the family with *SAMHD1* gene mutation associated with cerebral vasculopathy. Filled symbols represent affected individuals, and open symbols represent unaffected individuals. Circles and squares denote females and males, respectively. A double line identifies consanguinity. Arrows indicate affected individuals included in the genetic mapping study and sequence analysis.

pothyroidism, and glaucoma, although less common, had been found in at least three patients (Table 1).

The variations of cognitive and motor function development in these patients were striking. Four severely affected children manifested with profound global developmental delays and were completely dependent on their caregivers, whereas five patients demonstrated typical development without intellectual disability and participated in regular school. Three of them worked as

Table 1. Clinical features of 14 patients with the homozygous mutation in *SAMHD1* gene

Features	Incidence, % or average age
Neonatal features	
Mild intrauterine growth restriction (<15th percentile)	93 (13/14)
Underdeveloped (thin and transparent) skin at birth	50 (7/14)
Severe infantile irritability	62 (8/13)
Hypotonia	54 (7/13)
Failure to thrive	85 (11/13)
Short stature (<5th percentile)	92 (12/13)
Poor tolerance to extreme (cold and hot) environments	85 (11/13)
Acrocyanosis of hands, feet and face	85 (11/13)
Raynaud's phenomenon	85 (11/13)
Chilblain lesions in acral locations	62 (8/13)
Age of onset	5 y (1–7)
Low-pitch hoarse voice	90 (9/10)
Age of onset	7 y (3–12)
High-arched palate	85 (11/13)
Glaucoma	23 (3/13)
Migraine headache	30 (3/10)
Seizure	38 (5/13)
Hypothyroidism	23 (3/13)
Joint stiffness or arthritis	77 (10/13)
Scoliosis	46 (6/13)
Hemorrhagic stroke	
Confirmed	54 (7/13)
Suspected	15 (2/13)
Cognitive development	
Severely delayed	31 (4/13)
Mildly delayed	31 (4/13)
Normal	38 (5/13)
Elevated erythrocyte sedimentation rate (ESR)	82 (9/11)
Hyperimmunoglobulin G	83 (5/6)
Elevated neopterin	100 (3/3)

Incidence is expressed as a percentage with the number of patients applied in parentheses. The numbers in parentheses behind average age are ranges.

Table 2. Additional clinical features in individual patient with the homozygous mutation in *SAMHD1* gene

Patient	Sex	Initial presentation	Age at study, y	Ht at study, cm (per)	Other significant clinical history	Neuroimaging study findings					
						WM change	Aneurysms	Stenoses	Ischemic change	Volume loss	Age at imaging, y
X-1	M	FTT, chilblain	18	142 (<1)	Recovered from aneurysmal rupture at 17 y old, now farming	Mild–mod	+	+	–	–	17
X-3	M	FTT, chilblain	13	131 (<1)	Normal schooling	Mild–mod	–	–	–	–	12
X-4	M	FTT, chilblain	11	119 (<1)	Normal schooling	Mod	–	–	–	Mild	11
X-13	M	FTT, mild DD	12, died	125 (<1)	Glaucoma, died from recurrent strokes	Mod–severe	–	MM	+	Mild	12
X-15	F	FTT, mild DD	13, died	139 (<1)	Glaucoma, died from recurrent strokes	Severe	+	+	–	–	13
X-16	M	FTT, mild DD	10	119 (<1)	History of stroke	Mod	–	MM	+	Mild–Mod	8
X-19	F	CP, severe DD	25	N/A	History of possible stroke, severe spasticity						
X-27	M	arthritis	21	168 (10)	Working as a carpenter	–	–	+	–	–	20
X-28	M	arthritis	17	160 (2)	Working as a carpenter	–	–	MM	–	Mild	16
X-29	F	CP, severe DD	15	122 (<1)	History of possible stroke, glaucoma, spasticity	Mod	N/A	N/A	–	Mild–Mod	4
X-33	M	stroke	9	104 (<1)	Stroke at 5 mo old, recurrent strokes, spasticity	Mod–severe	–	MM	+	–	0.5
X-34	M	stroke	8	116 (2)	Stroke at 11 mo old	Mild–mod	N/A	N/A	–	Mild	5
X-35	F	stroke	2	71 (<1)	Stroke at 3 mo old						
X-38	M	none	Newborn	48 (25)	Found through requested DNA testing						

Per, percentile; Ht, height; WM, white matter; M, male; F, female; FTT, failure to thrive; DD, developmental delay; CP, cerebral palsy; mod, moderate; MM, moyamoya pattern; +, present; –, negative finding; N/A, no data are available.

farmers or carpenters when they reached their adulthood. It was noted that all eight patients with cognitive disability had a history of strokes, and for the four severely affected patients, the onset of stroke occurred during their early infancy. In fact, intracranial hemorrhagic strokes were documented in nine patients between the ages of 3 mo and 17 y, with five of them having recurrent cerebral events. The neurological outcomes were poor if the strokes occurred during early infancy as patients often became full-time wheelchair users with progressing spasticity and contracture of extremities over time. Likewise, the recurrent strokes were often associated with severe outcomes as both deceased patients died from recurrent strokes (Tables 1 and 2). Neither hypertension nor significantly abnormal hepatic and renal functions were documented in these patients.

Abnormal neuroimaging findings were identified in all 11 patients with available imaging studies such as magnetic resonance imaging (MRI) and magnetic resonance angiogram (MRA) and computed tomography (CT) and CT angiogram (CTA) (Fig. 2

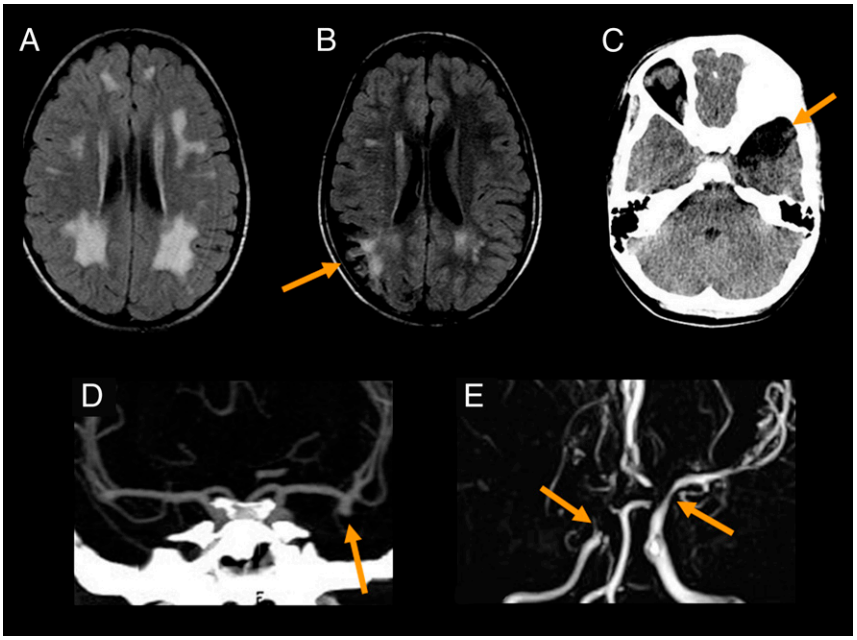

Fig. 2. Spectrum of neuroimaging abnormalities associated with the cerebral vasculopathy caused by *SAMHD1* gene mutation. (*A*) Axial FLAIR image from X-4 shows moderate nonspecific white matter signal hyperintensity, which is abnormal for age. The territory matches the internal–external watershed, which is vulnerable to chronic small vessel disease as often seen in elderly patients. (*B*) Axial FLAIR image from X-16 shows encephalomalacia from a prior right parietal transcortical infarct (arrow), with subcortical gliosis. Additional white matter change is present in the left periventricular regions, likely from chronic small vessel disease. (*C*) Axial noncontrast CT in X-15 shows encephalomalacia in the left anterior temporal lobe (arrow) from a preceding hemorrhagic stroke. (*D*) Coronal CTA from X-1 shows a large aneurysm arising from the left MCA bifurcation (arrow), projecting inferiorly. (*E*) Coronal maximal-intensity projection (MIP) from an MRA from X-28 shows extensive stenoses, severe in the right MCA territory with an acute cutoff (*Left* arrow) and minimal distal flow-related enhancement. There are similar stenoses in the bilateral A1 segments and a moderate stenosis of the distal left internal carotid artery (*Right* arrow).

and Table 2, and Fig. S1). All patients showed some degree of chronic ischemic change, manifested as abnormally increased T2/FLAIR white matter signal. The next most common finding, observed in seven out of nine MRAs and CTAs, was multifocal stenosis of the large intracranial arteries, namely the distal internal carotid artery, proximal middle cerebral artery (MCA), and anterior cerebral artery. Four patients showed stenoses severe enough to suggest a frank moyamoya pattern. Several studies revealed earlier frank acute infarction, both local and territorial. Two patients showed saccular aneurysms arising from the large vessels, particularly the MCA bifurcation. A marked increase in aneurysm size over an interval of 18 mo was observed in one patient. In addition, one patient showed encephalomalacia from a prior frank intracranial hemorrhage, and one showed subtle hemosiderin from a prior petechial hemorrhage. Postmortem examination of patient X-13 in the pedigree of Fig. 1 suggested early cerebral atherosclerosis, intimal proliferation, mild leukoencephalopathy, cerebellar hemorrrhage, and optic atrophy (Fig. S2).

Elevated erythrocyte sedimentation rate (ESR) (41 ± 33 mm/h) was observed in 11 patients, and increased serum IgG (2,331 ± 777 mg/dL) was detected in 6 patients. Abnormally increased serum neopterin level was also noted in all 3 patients tested (19.5 ± 4.4 nmol/L) (Table 1 and Table S2). In addition, mildly elevated anticardiolipin antibodies and antithyroglobulin antibodies were found in 2 patients (2/6), a positive rheumatoid factor was noted in 1 patient (1/4), whereas several other serum markers, such as C-reactive protein and antinuclear antibody C3 and C4, were in the normal range (Table S2). Furthermore, higher levels of serum tumor necrosis factor-α (TNF-α) were observed in affected individuals (17.4 ± 6.7 pg/mL, $n = 9$) compared with normal controls from the same community (10.3 ± 5.2 pg/mL, $n = 18$) ($P < 0.01$).

Genotyping and Mapping. To determine the genetic basis of this condition, we performed a genomewide autozygosity mapping study using Affymetrix GeneChip Mapping 10K SNP arrays with six affected individuals from three different sibships in the large consanguineous pedigree (Fig. 1). This mapping study was more difficult than previous studies due to the paucity of SNPs in the disease gene interval. Our initial analyses using all six patients failed to conclusively identify a single large homozygous region. The genotype data were then analyzed by assessing genotype identity (identity by state) between affected members within two families. Four genomic regions (on chromosomes (Chr) 2, 10, 14, and 20) demonstrated identity by state between affected members within each family. On the basis of these data, homozygosity was assessed within the families with respect to the four blocks of genotype identity. In the first family with three affected individuals, a single large shared homozygous region consisting of 23 contiguous SNPs was identified on chromosome 20q11.22-q12 (Fig. S3*A*). This shared homozygous block was 12.6 Mb in length and was bounded by SNPs rs721220 and rs1040546. In the second family with two affected individuals, multiple homozygous blocks were identified, one of which overlapped with the large block from the first family on chromosome 20. The overlapping interval, delimited by SNPs rs721220 and rs728331, further narrowed the candidate region to 8.9 Mb. Finally, examination of the single patient from the third family revealed a modest shared homozygous block of 8 SNPs in all patients (Fig. S3*B*). Examination of the minimal shared region, which was flanked by SNPs rs7259085 and rs728331, revealed 81 known or predicted genes based on both the NCBI and Celera annotations (Table S3).

Mutation Identification. Assessment of the 81 genes in the putative disease locus revealed 24 were predicted or hypothetical genes and 15 were pseudogenes. We prioritized sequence screening to the remaining 42 genes with known function or with sequence information validated in GenBank. Candidate gene sequencing was performed to screen the coding region and associated intronic splice junctions using genomic DNA from one patient. We sequenced five genes (*ADIG*, *FAM83D*, *GHRH*, *PPP1R16B*, and *SLC32A1*) before we identified a homozygous splice-acceptor site mutation (c.1411-2A > G) in intron 12 of the *SAMHD1* gene (Fig. 3*A*). The targeted sequencing of *SAMHD1* intron 12 and exon 13 boundary revealed that all affected individuals ($n = 14$) were homozygous for the mutation, their parents were heterozygous, and no unaffected siblings ($n = 21$) were homozygous for the change. We next screened 134 healthy Amish control samples ($n = 268$ chromosomes) from the same geographic area where the patients were found and determined that none were homozygous, whereas 4 were heterozygous for the c.1411-2A > G mutation (estimated carrier frequency of 3.0%). Further mutation screening for the DNA bank of the undiagnosed patients ($n = 44$), mostly with developmental delay in our institution, identified 3 more c.1411-2A > G homozygotes, raising the total number of affected individuals to 17. Review of their clinical history revealed a phenotype very similar to the 14 patients initially identified, with two infant patients being hypotonic and severely irritable, and the third one (9 y old) with a diagnosis of cerebral palsy with abnormal brain MRI in the past.

RNA Analysis. To investigate the consequence of this splice site mutation at the transcript level, we performed RT-PCR using RNA extracted from EBV-transformed lymphoblastoid cell lines with different c.1411-2A > G genotypes. This showed an aberrant shorter transcript from cell lines of affected individuals compared with the normal controls, whereas both normal and the aberrant transcripts were detected from heterozygous carriers (Fig. 3*B*). Direct sequencing of the PCR products after gel extraction revealed skipping of exon 13 (93 bp) in the abnormal transcript, which led to an in-frame deletion of 31 amino acids in translation (p.Glu471_Asp501del) (Fig. 3*C*).

Protein Analysis. Immunoblotting assays were performed with a polyclonal antibody raised against the full-length SAMHD1 protein and cell lysates prepared from lymphoblastoid cell lines. A protein band corresponding to wild-type SAMHD1 (~71 kDa) was detected from cell lines of a normal control and heterozygous carrier, but not the affected subject (Fig. 3*D*). Surprisingly, the mutant protein was barely detected from either the carrier or affected subject. Even after a prolonged exposure, only a faint band corresponding to the mutant SAMHD1 (p.Glu471_Asp501del) was observed in the cell lysate from the affected subject (Fig. 3*D*). Meanwhile, a trace amount of degraded SAMHD1 product was also observed in the affected subject, but not from the normal control (Fig. 3*D*).

Discussion

Here we describe an autosomal recessive condition manifesting with cerebral vasculopathy and early onset of stroke in an extended Old Order Amish pedigree. The patients seem affected during the early stage of development, even before they are born. Three full-term stillbirths are noted in two of the five affected families. The live newborns affected with this condition were relatively smaller, with thin, transparent, underdeveloped skin at birth, followed by hypotonia and severe irritability during early infancy.

Cerebral vasculopathy is a major hallmark found in all affected individuals with a common theme of stenoses and aneurysms. Typical neuroimaging findings include chronic ischemic changes, multifocal stenoses of the large intracranial arteries, including some with moyamoya morphology and evidence of prior acute infarction and hemorrhage. Migraine headaches might result from cerebral vasculopathy, whereas seizures seem to be a consequence of strokes as no patient had epilepsy documented before stroke. Ruptured aneurysms likely cause the most acute and severe outcomes. Progressive stenoses likely cause more chronic changes, starting with white matter gliosis in the deep watershed regions of the brain, where lower physiologic perfusion causes increased susceptibility to microischemia from any further reduction of perfusion pressure. With the progression of stenosis, the risk of catastrophic territorial

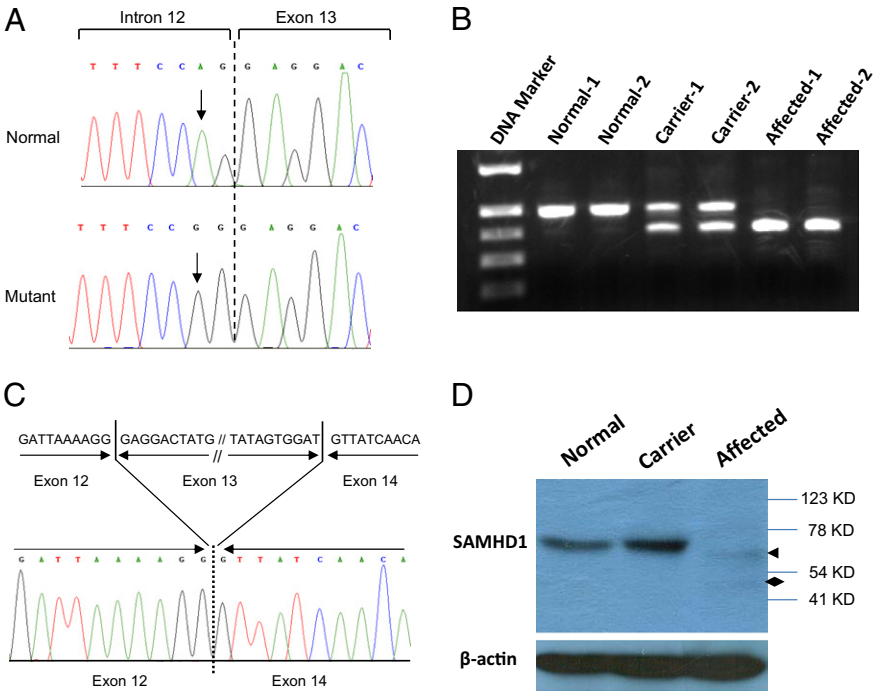

Fig. 3. Identification of the disease-causing mutation in *SAMHD1* gene. (*A*) Sequence electropherograms showing the homozygous c.1411-2A > G mutation from affected individuals compared with a normal control. (*B*) Agarose gel electrophoresis of RT-PCR products from lyphoblastoid cells showing a shorter abnormal transcript as a consequence of c.1411-2A > G mutation. (*C*) Sequencing analysis of the RT-PCR products showing the splicing out of exon 13 in the aberrant transcript. (*D*) Western blot analysis of SAMHD1 protein expression in cell line samples. Cell lysates of lymphoblastoid cell lines from a normal control, a carrier, and an affected individual were immunoblotted with anti-SAMHD1 antibody. An arrow indicates the trace amount of mutant SAMHD1 detected. A diamond shows a smaller weak band suggesting protein degradation of the mutant SAMHD1. β-Actin levels were monitored by immunoblotting as a control of protein loading.

infarction increases. Indeed, it has been noted that the clinical outcomes in these patients seem largely dependent on the degree of the cerebral vasculopathy, particularly if a stroke has occurred before evaluation. The early onset or recurrence of strokes seems associated with poor outcomes and variable cognitive disability, whereas patients without a history of stroke, although in a guarded condition, show fairly normal development without intellectual or motor disability. The phenotypic heterogeneity noted in this condition caused by the identical single mutation is remarkable, particularly considering the relatively uniform genetic background of the Amish population. We speculate that the time and location of catastrophic cerebral events in affected individuals may be largely responsible for such phenotype variation, implying a potential for proactive interventions. Thus, periodic cerebral angiograms as routine follow-up seem warranted for these patients as some vascular stenoses and aneurysms may be highly treatable with surgical procedures.

The clinical diagnosis of the disease remains challenging, particularly before the phenotype is described. This was well exemplified by unexpected diagnosis of three new patients through targeted sequencing of *SAMHD1* intron 12 and exon 13 boundary among undiagnosed patients with developmental delay in our institution. Indeed, the clinical features of this condition overlap with many assorted conditions such as congenital infection, cerebral palsy, moyamoya, vasculitis, lupus, rheumatoid arthritis, mixed connective-tissue disease, and primary angiitis of the central nervous system. It is noted that the pathological vascular changes are fairly organ specific, primarily notable in the brain and skin. Other than the many clinical and radiological findings related to cerebral vasculopathy found in these patients, acrocyanosis, Raynaud's phenomenon, and chilblain lesions in hands, feet, and face during winter are fairly characteristic of this condition. These clinical features might be a reflection of pathological vascular changes in skin. Interestingly, other essential organs are not notably affected as all patients have normal blood pressure and normal cardiac, hepatic, and renal functions. Although the specific relationship between abnormal skin and cerebral vasculopathy remains to be understood, these rare dermatological manifestations seem fairly disease specific. We wonder whether these clinical features could potentially serve for identification of affected individuals in the general population.

Through genomewide homozygosity mapping and mutational analysis in affected individuals from a consanguineous pedigree, we have identified a pathogenic sequence variant, c.1411-2A > G, in the *SAMHD1* gene that is associated with the disease. This alteration has not been reported as a polymorphic variant in GenBank. It cosegregates consistently with the disease phenotype, as all affected individuals are homozygous, their parents are heterozygous, and no unaffected siblings or normal controls are homozygous for the mutation. The *SAMHD1* gene consists of 16 coding exons and encodes a protein of 626 amino acids. The c.1411-2A > G mutation, appeared at the consensus splice-acceptor site in intron 12, resulted in skipping of exon 13 of mRNA transcript, and gave rise to an aberrant protein with in-frame deletion of 31 amino acids (p.Glu471_Asp501del). Although RT-PCR showed robust expression of aberrant *SAMHD1* mRNA transcript in affected cell lines, the mutated form of SAMHD1 protein was barely detected by Western blot from those cells, suggesting that the lack of SAMHD1 protein expression might be due to protein degradation or reflects impaired protein translation. The results further indicate that the disease pathogenesis likely reflects a loss of SAMHD1 protein rather than expression of a partially functional protein.

Little is known about the function of SAMHD1. SMART sequence analysis shows two functional domains in SAMHD1 protein: a sterile alpha motif (SAM) (residuals 42–110) and an HD domain (residuals 160–325). The SAM domain is a putative protein interaction module mediating interactions with other SAM domain and non-SAM domain-containing proteins (4). In addition, SAM domains also appear to possess the ability to bind RNA (5). The HD domain is found in a superfamily of enzymes with a predicted or known phosphohydrolase activity appearing to be involved in the nucleic acid metabolism (6). This evidence suggests that SAMHD1 may act as a nuclease. Mutations in the *SAMHD1* gene have recently been identified as one of five causative agents for a rare genetic condition, Aicardi-Goutières syndrome (7, 8), highlighting the presence of different pathogenic mutations in the SAMHD1 gene beyond the Amish population. However, the phenotype reported here is apparently incompatible with Aicardi-Goutières syndrome, which is a type of encephalopathy whose clinical features mimic those of acquired in utero viral infection. Furthermore, none of our 17

patients has been diagnosed with Aicardi-Goutières syndrome. The wide spectrum of the disease phenotype caused by *SAMHD1* mutation reported here indicates a potentially much broader implication of this study. In fact, *SAMHD1* was originally identified in a human dendritic cell cDNA library as an ortholog of the mouse IFN-γ–induced gene *Mg11* and even termed dendritic cell derived IFN-γ–induced protein (DCIP) (9). Several lines of evidence implicate SAMHD1 in immune function as it is upregulated in response to viral infections and may have a role in mediating TNF-α proinflammatory responses (10–13). A more recent study suggests that SAMHD1 may act as a negative regulator of the immunostimulatory DNA response and may have a protective role in preventing self-activation of innate immunity (7). Indeed, many clinical findings in our report, particularly abnormal laboratory findings (e.g., elevated ESR, IgG, neopterin, and TNF-α) in the patients support a particular role for SAMHD1 as an immunomodulator.

It is noted that innate and adaptive immune processes are involved in medium- and large-vessel vasculitis (14–17). The vasculopathy associated with *SAMHD1* mutation in this study consistently targets certain organs while sparing others. Remarkable target tissue tropisms with distinctive vascular territories have been observed in several other inflammatory vasculopathies related to their vessel-specific Toll-like receptor (TLR) profile (18–20). We speculate that SAMHD1 may play an important role in cerebral vasculopathy, and further studies of the role of SAMHD1 in blood vessel integrity and homeostasis of the brain will be very significant not only for this condition, but for a group of diseases related to cerebral vasculopathies, such as moyamoya (21) and primary angiitis of the central nervous system (22).

Materials and Methods

Subjects and Clinical Assessment. The study was approved by the DDC Clinic for Special Needs Children Institutional Review Board, and written informed consent was obtained from each participant or their legal guardian. A total of 14 affected individuals from four separate Old Order Amish settlements in Ohio, Kentucky, and Tennessee were clinically evaluated. Additional clinical information and neuroimaging studies obtained through the medical records were reviewed. The diagnosis was established on the basis of family history, physical examination, laboratory results and imaging studies, and later confirmed by DNA mutation analysis. Most parents and siblings of the patients also chose to participate in the study. Plasma TNF-α, as a part of HumanMAP antigen panel, was measured using fully automated, bead-based multiplex sandwich immunofluorescence assays provided by Rules-Based Medicine in nine affected individuals and 18 normal controls of the same ethnic background and age range. The genealogical information obtained from the affected families was confirmed and expanded through the Swiss Anabaptist Genealogical Association.

Genotyping and Mutation Detection. DNA isolation, genotyping, and mutation detection were performed as described previously (23, 24). PCR primers were designed to amplify each of the 16 protein-coding exons and their flanking intronic sequences of *SAMHD1*. Primer sequences are provided in Table S4. The GenBank accession nos. of both genomic DNA and mRNA reference sequences used in this study are NT_011362 and NM_015474, respectively.

Reverse Transcription-PCR. Total RNA was isolated from EBV-transformed lymphoblastoid cell lines using QIAamp RNA kit (Qiagen) according to the manufacturer's protocol. cDNA was synthesized by priming of 5 μg of total RNA using SuperScript First-Strand Synthesis system (Invitrogen) following the manufacturer's protocol. PCR amplification of *SAMHD1* cDNA was performed using primers F1231 and R1726 located in exons 11 and 15, respectively (Table S4, the base pair numbers of primers were determined according to the mRNA sequence NM_015474). The amplicons were analyzed by agarose gel electrophoresis, purified on Qiaquick spin columns, and sequenced by Big Dye terminator cycle sequencing.

Protein Analysis. Lymphoblastoid cell lines from peripheral blood samples were prepared and maintained using standard techniques. Total cell lysates were prepared by incubating cells at 4 °C for 30 min in the Nonidet P-40 lysis buffer supplemented with protease inhibitors. Lysates were centrifuged for 10 min at 14,000 rpm at 4 °C, and the clarified supernatants were then loaded onto SDS polyacrylamide gels. After SDS/PAGE, proteins were transferred onto polyvinylidene difluoride membranes (Millipore). Membranes were blocked for 1 h with 5% nonfat milk and incubated overnight at 4 °C with a 1:500 dilution of mouse anti-SAMHD1 polyclonal antibody (Sigma-Aldrich). The following day, the blots were washed 3 × 10 min with PBS/0.2% Tween-20 and then incubated for 1 h at room temperature with a 1:2,000 dilution of horse antimouse IgG horseradish peroxidase (Cell Signaling Technology). After washing with PBS/0.2% Tween-20, the protein bands were detected by ECL chemiluminescent assay (GE Healthcare).

Statistical Analysis. All data are presented as means ± SD. Comparisons of the affected individuals and controls were made using Student's *t* test and *P* value <0.05 was considered statistically significant.

ACKNOWLEDGMENTS. We thank the families for their patience and support. We appreciate the physicians who provided outstanding and compassionate care to the affected children through Rainbow Babies and Children's Hospital, Cincinnati Children's Hospital Medical Center, Kosair Children's Hospital, Vanderbilt University Medical Center, and Shriners Hospitals for Children, and Carol Troyer, Carol Nelson, and Betty Presler who helped with the data collection. The study was supported in part by the Elisabeth Severance Prentiss Foundation, the Reinberger Foundation, and the Leonard Krieger Fund of the Cleveland Foundation (L2009-0078).

1. Pappachan J, Kirkham FJ (2008) Cerebrovascular disease and stroke. *Arch Dis Child* 93: 890–898.
2. Seidman C, Kirkham F, Pavlakis S (2007) Pediatric stroke: Current developments. *Curr Opin Pediatr* 19:657–662.
3. Francis J, Raghunathan S, Khanna P (2007) The role of genetics in stroke. *Postgrad Med J* 83:590–595.
4. Schultz J, Ponting CP, Hofmann K, Bork P (1997) SAM as a protein interaction domain involved in developmental regulation. *Protein Sci* 6:249–253.
5. Kim CA, Bowie JU (2003) SAM domains: Uniform structure, diversity of function. *Trends Biochem Sci* 28:625–628.
6. Aravind L, Koonin EV (1998) The HD domain defines a new superfamily of metal-dependent phosphohydrolases. *Trends Biochem Sci* 23:469–472.
7. Rice GI, et al. (2009) Mutations involved in Aicardi-Goutières syndrome implicate SAMHD1 as regulator of the innate immune response. *Nat Genet* 41:829–832.
8. Ramesh V, et al. (2010) Intracerebral large artery disease in Aicardi-Goutières syndrome implicates SAMHD1 in vascular homeostasis. *Dev Med Child Neurol* 52:725–732.
9. Li N, Zhang W, Cao X (2000) Identification of human homologue of mouse IFN-gamma induced protein from human dendritic cells. *Immunol Lett* 74:221–224.
10. Hartman ZC, et al. (2007) Adenovirus infection triggers a rapid, MyD88-regulated transcriptome response critical to acute-phase and adaptive immune responses in vivo. *J Virol* 81:1796–1812.
11. Préhaud C, Mégret F, Lafage M, Lafon M (2005) Virus infection switches TLR-3-positive human neurons to become strong producers of beta interferon. *J Virol* 79:12893–12904.
12. Zhao D, Peng D, Li L, Zhang Q, Zhang C (2008) Inhibition of G1P3 expression found in the differential display study on respiratory syncytial virus infection. *Virol J* 5:114.
13. Liao W, Bao Z, Cheng C, Mok YK, Wong WS (2008) Dendritic cell-derived interferon-gamma-induced protein mediates tumor necrosis factor-alpha stimulation of human lung fibroblasts. *Proteomics* 8:2640–2650.
14. Millonig G, Schwentner C, Mueller P, Mayerl C, Wick G (2001) The vascular-associated lymphoid tissue: A new site of local immunity. *Curr Opin Lipidol* 12:547–553.
15. Weyand CM, Goronzy JJ (2003) Medium- and large-vessel vasculitis. *N Engl J Med* 349: 160–169.
16. Wick G, Knoflach M, Xu Q (2004) Autoimmune and inflammatory mechanisms in atherosclerosis. *Annu Rev Immunol* 22:361–403.
17. Han JW, et al. (2008) Vessel wall-embedded dendritic cells induce T-cell autoreactivity and initiate vascular inflammation. *Circ Res* 102:546–553.
18. Hoffman GS (2005) Determinants of vessel targeting in vasculitis. *Ann N Y Acad Sci* 1051:332–339.
19. Pryshchep O, Ma-Krupa W, Younge BR, Goronzy JJ, Weyand CM (2008) Vessel-specific Toll-like receptor profiles in human medium and large arteries. *Circulation* 118:1276–1284.
20. Deng J, et al. (2009) Toll-like receptors 4 and 5 induce distinct types of vasculitis. *Circ Res* 104:488–495.
21. Scott RM, Smith ER (2009) Moyamoya disease and moyamoya syndrome. *N Engl J Med* 360:1226–1237.
22. Hajj-Ali RA, Calabrese LH (2009) Central nervous system vasculitis. *Curr Opin Rheumatol* 21:10–18.
23. Puffenberger EG, et al. (2004) Mapping of sudden infant death with dysgenesis of the testes syndrome (SIDDT) by a SNP genome scan and identification of TSPYL loss of function. *Proc Natl Acad Sci USA* 101:11689–11694.
24. Xin B, et al. (2010) Homozygous frameshift mutation in *TMCO1* causes a syndrome with craniofacial dysmorphism, skeletal anomalies, and mental retardation. *Proc Natl Acad Sci USA* 107:258–263.